Static and Dynamic Analysis of Hyperboloidal Helix Having Thin Walled Open and Close Sections

Merve Ermis, Murat Yılmaz, Nihal Eratlı, Mehmet H. Omurtag

Abstract—The static and dynamic analyses of hyperboloidal helix having the closed and the open square box sections are investigated via the mixed finite element formulation based on Timoshenko beam theory. Frenet triad is considered as local coordinate systems for helix geometry. Helix domain is discretized with a two-noded curved element and linear shape functions are used. Each node of the curved element has 12 degrees of freedom, namely, three translations, three rotations, two shear forces, one axial force, two bending moments and one torque. Finite element matrices are derived by using exact nodal values of curvatures and arc length and it is interpolated linearly throughout the element axial length. The torsional moments of inertia for close and open square box sections are obtained by finite element solution of St. Venant torsion formulation. With the proposed method, the torsional rigidity of simply and multiply connected cross-sections can be also calculated in same manner. The influence of the close and the open square box cross-sections on the static and dynamic analyses of hyperboloidal helix is investigated. The benchmark problems are represented for the literature.

Keywords—Hyperboloidal helix, squared cross section, thin walled cross section, torsional rigidity

I. INTRODUCTION

HELICOIDAL bars are important and frequently used members in civil engineering, mechanical engineering and biomechanics. They have many different forms other than their well known standard form. They have the ability to absorb energy while deforming. Although a tremendous amount of theoretical and numerical studies exists on the static/dynamic analyses of elastic helixes, it can be observed that only helices with limited number of cross-sections (e.g., circular and rectangular) were considered. The static analysis with rectangular cross-section [1]-[3], and, the dynamic analysis with circular cross section [4]-[7], thin-thick walled circular cross section [8], and rectangular cross-section [9] are studied.

It is straightforward to calculate the torsional rigidity of helices having a circular cross section. In the case of non-circular geometries, some special treatments have to be used to determine the torsional rigidity. It is possible to find some analytical formulas in the literature expressing the torsional moment of inertia for various arbitrary cross-sections like rectangular, ellipse and equilateral triangle [10]. Some approximated analytical formulas [11], [12] and numerical

M. Ermis, M. Yılmaz, N. Eratlı, M. H. Omurtag, are with the Faculty of Civil Engineering, Istanbul Technical University, Maslak 34469, Turkey (phone: +90-212-2856551; e-mail: ermism@itu.edu.tr, e-mail: yilmazmura@itu.edu.tr, e-mail: eratli@itu.edu.tr, e-mail: omurtagm@itu.edu.tr).

solutions such as finite difference [13], [14], finite element (FE) [15]-[20], and boundary element methods also exist [21], [22].

In this study, the effects of the noncircular cross-sections on the static and dynamic behavior of hyperboloidal helix are considered. The torsional rigidities of used cross-sections are calculated by FE solution of Poisson's equation proposed by [20]. The mixed FE formulation comprising the Timoshenko beam theory is employed. As a numerical investigation, the influence of the cross-sections and the boundary conditions on the static and dynamic analyses of the hyperboloidal helix is performed via the mixed FE method.
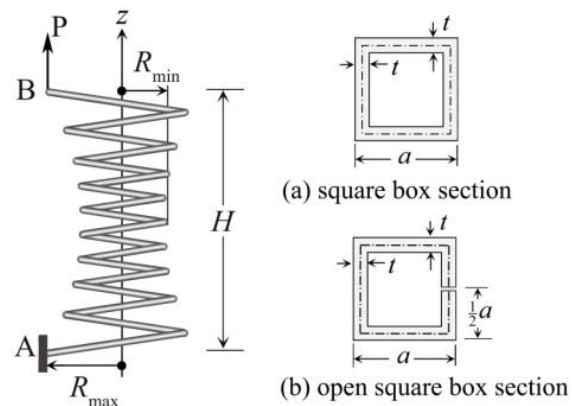

Fig. 1 Hyperboloidal helix and cross-sections

II. FORMULATION

A. Helix Geometry and Functional

The geometrical properties of the helix are $x = R(\varphi)\cos\varphi$, $y = R(\varphi)\sin\varphi$, $z = p(\varphi)\varphi$, $p(\varphi) = R(\varphi)\tan\alpha$, where α denotes the pitch angle, $R(\varphi)$ and $p(\varphi)$ signify the centerline radius and the step for unit angle, respectively, of the helix as a function of the horizontal angle φ. By letting $c(\varphi) = \sqrt{R^2(\varphi) + p^2(\varphi)}$, the infinitesimal arc length becomes $ds = c(\varphi)\,d\varphi$. In the case of a hyperboloidal helix, its radius

$$R(\varphi) = R_{\min} + (R_{\max} - R_{\min})\,(1 - \varphi/n\pi)^2 \qquad (1)$$

where $R_{\max}$ and $R_{\min}$ are the bottom radius and the central radius, respectively (see Fig. 1).

The field equations for the elastic circular and non-circular helices, which are based on Timoshenko beam theory and

refer to the Frenet coordinate system, exist in [20], these equations can be written in the form

$$-\mathbf{T}_{,s} - \mathbf{q} + \rho A\ddot{\mathbf{u}} = \mathbf{0} \ \Big\} $$
$$-\mathbf{M}_{,s} - \mathbf{t}\times\mathbf{T} - \mathbf{m} + \rho\mathbf{I}\ddot{\boldsymbol{\Omega}} = \mathbf{0} \ \Big\} \qquad (2)$$

$$\mathbf{u}_{,s} + \mathbf{t}\times\boldsymbol{\Omega} - \mathbf{C}_{\gamma}\mathbf{T} = \mathbf{0} \ \Big\} $$
$$\boldsymbol{\Omega}_{,s} - \mathbf{C}_{\kappa}\mathbf{M} = \mathbf{0} \ \Big\} \qquad (3)$$

where $\mathbf{u}(u_t, u_n, u_b)$ is the displacement vector, $\boldsymbol{\Omega}(\Omega_t, \Omega_n, \Omega_b)$ is the rotational vector, $\mathbf{T}(T_t, T_n, T_b)$ is the force vector, $\mathbf{M}(M_t, M_n, M_b)$ is the moment vector. $\ddot{\mathbf{u}}$ and $\ddot{\boldsymbol{\Omega}}$ are the accelerations of the displacement and rotations. ρ is the material density. A is the area of the cross section, $\mathbf{I}$ is the moments of inertia, $\mathbf{C}_{\gamma}$ and $\mathbf{C}_{\kappa}$ are compliance matrices. $\mathbf{q}$ and $\mathbf{m}$ are the distributed external force and moment vectors, respectively. In the dynamic analysis, the motion is considered as harmonic and the conditions $\mathbf{q} = \mathbf{m} = \mathbf{0}$ are satisfied. Incorporating Gâteaux differential with potential operator concept [23] yields the functional in terms of (2), (3)

$$\mathbf{I}(\mathbf{y}) = -\left[\mathbf{u}, \frac{d\mathbf{T}}{ds}\right] + [\mathbf{t}\times\boldsymbol{\Omega}, \mathbf{T}] - \left[\frac{d\mathbf{M}}{ds}, \boldsymbol{\Omega}\right] - \frac{1}{2}[\mathbf{C}_{\kappa}\,\mathbf{M}, \mathbf{M}]$$
$$- \frac{1}{2}[\mathbf{C}_{\gamma}\,\mathbf{T}, \mathbf{T}] - \frac{1}{2}\rho A\omega^2[\mathbf{u}, \mathbf{u}] - \frac{1}{2}\rho\,\omega^2[\mathbf{I}\boldsymbol{\Omega}, \boldsymbol{\Omega}]$$
$$- [\mathbf{q}, \mathbf{u}] - [\mathbf{m}, \boldsymbol{\Omega}] + \left[(\mathbf{T} - \hat{\mathbf{T}}), \mathbf{u}\right]_{\sigma} + \left[(\mathbf{M} - \hat{\mathbf{M}}), \boldsymbol{\Omega}\right]_{\sigma} \qquad (4)$$
$$+ [\hat{\mathbf{u}}, \mathbf{T}]_{\varepsilon} + [\hat{\boldsymbol{\Omega}}, \mathbf{M}]_{\varepsilon}$$

where square brackets indicate the inner product, the terms with hats are known values on the boundary and the subscripts ε and σ represent the geometric and dynamic boundary conditions, respectively.

B. Calculation of Torsional Rigidity via FEM

Let's Φ is a scalar field function. The governing equation for the torsion problem is

$$\Phi_{,11} + \Phi_{,22} = -2 \qquad (5)$$

with $\Phi = 0$ on Γ the boundary. Defining a vector field $\boldsymbol{\Xi}$ on Ω^e as $\boldsymbol{\Xi} = \{\psi_i\,\Phi^e_{,1}, \psi_i\,\Phi^e_{,2}\}^{\mathrm{T}}$ and using the divergence theorem the weak form of (5) can be constructed as,

$$\int_{\Omega^e}\left(\psi_{i,1}\,\Phi^e_{,1} + \psi_{i,2}\,\Phi^e_{,2}\right)d\Omega^e = 2\int_{\Omega^e}\psi_i\,d\Omega^e + \oint_{\Gamma^e}\psi_i\,\nabla\Phi^e\cdot\mathbf{n}^e d\Gamma^e \quad (6)$$

The boundary terms in (6) cancel out during the assemblage of the FE equations for adjacent element edges in the cross-section domain Ω and they are also zero on the free edges (edges without an adjacent element) to satisfy the boundary

condition of the torsion problem. The torsional constant I_t of the cross-section, in terms of the scalar field, is expressed as,

$$I_t = -\int_{\Omega}\left(\Phi_{,1}x_1 + \Phi_{,2}x_2\right)d\Omega \qquad (7)$$

which renders to the summation given with the following equation over domain elements as,

$$\mu I_3 = -\sum_{e=1}^{N}\mu^e\int_{\Omega^e_{\eta}}\boldsymbol{\Phi}^{\mathrm{T}}[\partial\boldsymbol{\psi}][\mathbf{J}]^{-1}[\mathbf{X}]\boldsymbol{\psi}\left|\det[\mathbf{J}]\right|d\Omega^e_{\eta} \qquad (8)$$

where $[\partial\boldsymbol{\psi}]$ with the definition,

$$[\partial\boldsymbol{\psi}] = \begin{bmatrix} \partial\psi_1/\partial\eta_1 & \partial\psi_1/\partial\eta_2 \\ \partial\psi_2/\partial\eta_1 & \partial\psi_2/\partial\eta_2 \\ \vdots & \vdots \\ \partial\psi_9/\partial\eta_1 & \partial\psi_9/\partial\eta_2 \end{bmatrix} \qquad (9)$$

where $[\mathbf{J}]$ (Jacobian matrix) is calculated with $[\mathbf{J}] = [\mathbf{X}][\partial\boldsymbol{\psi}]$, $[\mathbf{X}]$ being the nodal coordinates matrix, and $\boldsymbol{\Phi}$ is the vector with the scalar field nodal-values as its components. Integrations are performed with the $3\times 3 = 9$ point Gauss quadrature rule. $\mu = G$ is the shear modulus and N is the total number of elements.

C. The Mixed FE Method and Dynamic Analysis

$\phi_i = (\varphi_j - \varphi)/\Delta\varphi$ and $\phi_j = (\varphi - \varphi_i)/\Delta\varphi$ are linear shape functions used in FE formulation where $\Delta\varphi = (\varphi_j - \varphi_i)$. The subscripts represent node numbers of the curved element. The curvatures are satisfied exactly at the nodal points and linearly interpolated through the element. The curved bar element has two nodes with 2×12 degrees of freedom. The variable vectors per node are $\mathbf{u}, \boldsymbol{\Omega}, \mathbf{T}, \mathbf{M}$.

In the dynamic analysis, the problem of determining the natural frequencies reduces to the solution of a standard eigenvalue problem $([\mathbf{K}] - \omega^2[\mathbf{M}])\{\mathbf{u}\} = \{\mathbf{0}\}$ where $[\mathbf{K}]$ is the system matrix, $[\mathbf{M}]$ is the mass matrix $\mathbf{u}$ is the eigenvector (mode shape) and ω is the natural angular frequency of the system. Hence the explicit form of standard eigenvalue problem in the mixed formulation is

$$\left(\begin{bmatrix} [\mathbf{K}_{11}] & [\mathbf{K}_{12}] \\ [\mathbf{K}_{22}] & [\mathbf{K}_{22}] \end{bmatrix} - \omega^2\begin{bmatrix} [\mathbf{0}] & [\mathbf{0}] \\ [\mathbf{0}] & [\mathbf{M}] \end{bmatrix}\right)\begin{Bmatrix} \{\mathbf{F}\} \\ \{\mathbf{U}\} \end{Bmatrix} = \begin{Bmatrix} \{\mathbf{0}\} \\ \{\mathbf{0}\} \end{Bmatrix} \qquad (10)$$

where $\{\mathbf{F}\}$ denotes the nodal force and the moment vectors and $\{\mathbf{U}\} = \{\mathbf{u}\ \boldsymbol{\Omega}\}^T$ signifies the nodal displacement and rotation vectors. To attain consistency between (10) and $([\mathbf{K}] - \omega^2[\mathbf{M}])\{\mathbf{u}\} = \{\mathbf{0}\}$, the $\{\mathbf{F}\}$ is eliminated in (10), which yields to the condensed system matrix

$[\mathbf{K}^*]=[\mathbf{K}_{22}]-[\mathbf{K}_{12}]^{\mathrm{T}}[\mathbf{K}_{11}]^{-1}[\mathbf{K}_{12}]$. The eigenvalue problem in the mixed formulation becomes $\left([\mathbf{K}^*]-\omega^2[\mathbf{M}]\right)\{\mathbf{U}\}=\{\mathbf{0}\}$.

III. NUMERICAL EXAMPLES

The material and geometric properties of the hyperboloidal helix are: the modulus of elasticity is $E=210\,\mathrm{GPa}$, Poisson's ratio is $\upsilon=0.3$, the number of active turns is $n=7.5$, the height of the helix is $H=75\,\mathrm{mm}$, the ratio of the minor radius to the major radius of the helix is $R_{\min}/R_{\max}=0.5$ where $R_{\max}=13\,\mathrm{mm}$. Closed and open square box sections that range from thin to thick with four different thickness-to-side ratios t/a (0.040, 0.125, 0.250, 0.375) where $a=2\,\mathrm{mm}$ are employed (see Figs. 1 (a), (b)). The torsional rigidity moments of these closed and open sections are calculated via FE method which is verified in [20]. Referring to t/a (0.040, 0.125, 0.250, 0.375) ratios, the computed torsional inertia moments for closed square box section are $I_t=0.0366a^4$, $0.0923a^4$, $0.1305a^4$, $0.1399a^4$ and the computed torsional moments for open square box sections are $I_t=8.2\times10^{-5}a^4$, $229.6\times10^{-5}a^4$, $1589.2\times10^{-5}a^4$ and $4455.5\times10^{-5}a^4$, respectively.

A. Static Analysis

The behavior of the closed and open square box sections, ranging from thin to thick with four different thickness-to-side ratios, on the nodal variables at the specific points of the hyperboloidal helix are investigated. The fixed-free boundary condition is used. The helix is subjected to an external load acting at the tip of the helix (see Fig. 1, point B). The intensity of the load is $P_z=10^{-3}\,\mathrm{N}$. The hyperboloidal helix problem having thin and thick with four different t/a ratios of the closed and open square box sections are solved and the results are presented in the Cartesian coordinate system. The maximum displacements (u_z) and fixed end reactions (T_z: shear force, M_y: moment) for closed and open sections are tabulated in Tables I, II. These results are verified using the commercial program SAP2000and its Section Designer module.

In the closed square box cross-section, with respect to the maximum displacements for the $t/a=0.04$ ratio, the reductions for the next three t/a (0.125, 0.250, 0.375) ratios are 59.9%, 71.5% and 73.4% (Table I). Similarly, in the open square box cross-section, with respect to the maximum displacements for the $t/a=0.04$ ratio, the reductions for the next three ratios are 96.4%, 99.5% and 99.8% (Table II). It is observed that the open square box sections are more sensitive the changing of the thickness-to-side ratios (Tables I, II). For the maximum displacements of the helicoidal helix, the results of the closed square box section for each t/a ratio are decreased by 99.7%, 96.7%, 84.2%, and 61.2% with respect to the open square box cross-section results (Tables I, II).

TABLE I
THE DISPLACEMENTS, SHEAR FORCES AND MOMENTS OF HYPERBOLOIDAL HELIX HAVING THE THIN-THICK SQUARE BOX SECTIONS

t/a		$(u_z)_{\max}$ ($\times10^{-3}$ mm)	$(T_z)_{\max}$ ($\times10^{-4}$ N)	$(M_y)_{\max}$ ($\times10^{-5}$ Nm)
0.040	this study	1.955	9.983	2.591
	SAP2000	1.961	10.00	2.600
	diff.%	-0.31	-0.17	-0.35
0.125	this study	0.784	9.983	2.591
	SAP2000	0.789	10.00	2.600
	diff.%	-0.64	-0.17	-0.35
0.250	this study	0.557	9.983	2.591
	SAP2000	0.557	10.00	2.600
	diff.%	0.00	-0.17	-0.35
0.375	this study	0.520	9.983	2.591
	SAP2000	0.516	10.00	2.600
	diff.%	0.77	-0.17	-0.35

diff. % = (This study-SAP2000)×100/This study

TABLE II
THE DISPLACEMENTS, SHEAR FORCES AND MOMENTS OF HYPERBOLOIDAL HELIX HAVING THE THIN-THICK OPEN SQUARE BOX SECTIONS

t/a		$(u_z)_{\max}$ ($\times10^{-3}$ mm)	$(T_z)_{\max}$ ($\times10^{-4}$ N)	$(M_y)_{\max}$ ($\times10^{-5}$ Nm)
0.040	this study	653.7	9.983	2.591
	SAP2000	648.1	10.00	2.600
	diff.%	0.86	-0.17	-0.35
0.125	this study	23.55	9.983	2.591
	SAP2000	23.34	10.00	2.600
	diff.%	0.89	-0.17	-0.35
0.250	this study	3.520	9.983	2.591
	SAP2000	3.490	10.00	2.600
	diff.%	0.85	-0.17	-0.35
0.375	this study	1.340	9.983	2.591
	SAP2000	1.330	10.00	2.600
	diff.%	0.75	-0.17	-0.35

diff. % = (This study-SAP2000)×100/This study

B. Dynamic Analysis

The objective of this example is to investigate the effects of the thickness-to-side ratios of the closed and open sections and the boundary conditions on the dynamic behavior of the hyperboloidal helix. The fixed-fixed and fixed-free boundary conditions are employed. The density of material is $\rho=7850\,\mathrm{kg/m^3}$. For the fixed-fixed and the fixed free boundary conditions, the first six natural frequency results of the helicoidal helix having the closed and open sections are presented in Tables III-VI. The results are also verified with SAP2000 and its Section Designer module.

In the case of the fixed-fixed boundary condition and the closed square box section, with respect to the fundamental natural frequency for the $t/a=0.04$ ratio, the reductions for the next three t/a (0.125, 0.250, 0.375) ratios are 6.9%, 16.0% and 22.3% (Table III). Similarly, in the case of the fixed-free boundary condition and the closed square box section, with respect to the fundamental natural frequency for the $t/a=0.04$ ratio, the reductions for the next three t/a ratios are 6.7%, 15.7% and 22.1% (Table IV). In the case of the fixed-fixed boundary condition and the open closed square

box section, with respect to the fundamental natural frequency for the $t/a = 0.04$ ratio, the increases for the next three t/a ($0.125, 0.250, 0.375$) ratios are 213.3%, 527.2% and 831.2% (Table V). Similarly, in the case of the fixed-free boundary condition and the open closed square box section, with respect to the fundamental natural frequency for the $t/a = 0.04$ ratio, the increases for the next three t/a ratios are 208.1%, 500.0% and 748.6% (Table VI). For both closed and open square box sections, when the influence of the boundary conditions is considered the fundamental natural frequencies of the fixed-free boundary condition decreased in the range of 78.6%~81.3% with respect to the fixed-fixed boundary condition (Tables III-VI). For the fundamental natural frequency of the hyperboloidal helix having fixed-fixed boundary condition, the results of the open square box section for each t/a ratio are decreased by 94.7%, 82.2%, 60.4%, and 36.4% with respect to the closed square box cross-section results (Tables III, V). For the fundamental natural frequency of the hyperboloidal helix having fixed-free boundary condition, the results of the open square box section for each t/a ratio are decreased by 93.9%, 80.0%, 56.8%, and 33.9% with respect to the closed square box cross-section results (Tables IV, VI).

TABLE III
THE NATURAL FREQUENCIES OF HYPERBOLOIDAL HELIX HAVING THE THIN-THICK SQUARE BOX SECTIONS WITH FIXED-FIXED BOUNDARY CONDITION

| t/a		ω (in Hz)					
		1	2	3	4	5	6
0.04	this study	326.3	336.2	359.7	608.4	719.1	765.7
	SAP2000	326.0	335.1	356.2	608.6	717.6	764.4
	diff.%	0.09	0.33	0.97	-0.03	0.21	0.17
0.125	this study	303.8	312.5	338.0	560.3	668.1	711.2
	SAP2000	303.0	311.2	334.0	560.2	665.8	709.6
	diff.%	0.26	0.42	1.18	-0.04	0.34	0.22
0.25	this study	274.1	281.6	307.2	501.6	601.9	640.8
	SAP2000	274.2	281.3	305.3	501.4	601.2	641.1
	diff.%	-0.04	0.11	0.62	0.04	0.12	-0.05
0.375	this study	253.5	260.4	284.9	462.8	556.6	592.7
	SAP2000	254.0	260.5	284.2	462.4	556.6	593.7
	diff.%	-0.20	0.04	0.25	0.09	0.00	-0.17

diff. % = (This study-SAP2000)×100/This study
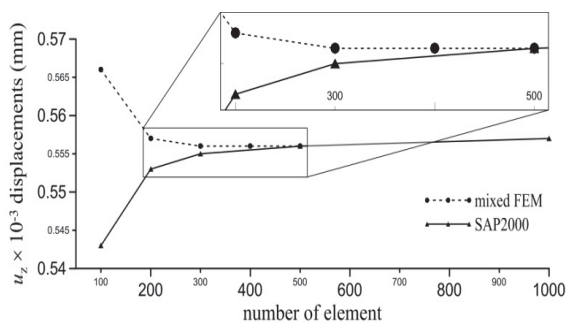
Fig. 2 The convergence analysis for u_z displacement of the hyperboloidal helix having square box cross-section with fixed-free boundary condition

TABLE IV
THE NATURAL FREQUENCIES OF HYPERBOLOIDAL HELIX HAVING THE THIN-THICK SQUARE BOX SECTIONS WITH FIXED-FREE BOUNDARY CONDITION

t/a		ω (in Hz)					
		1	2	3	4	5	6
0.040	this study	61.0	61.8	198.1	255.4	322.1	330.0
	SAP2000	60.8	61.6	196.6	255.2	321.6	328.8
	diff.%	0.33	0.32	0.76	0.08	0.16	0.36
0.125	this study	56.9	57.6	186.4	235.3	299.5	307.3
	SAP2000	56.6	57.2	184.5	235.1	298.6	305.7
	diff.%	0.53	0.42	1.18	-0.04	0.34	0.22
0.250	this study	51.4	51.9	169.6	210.7	270.0	277.3
	SAP2000	51.3	51.8	168.9	210.5	270.0	276.8
	diff.%	0.19	0.19	0.41	0.09	0.00	0.18
0.375	this study	47.5	48.0	157.4	194.4	249.7	256.5
	SAP2000	47.5	48.0	157.3	194.2	250.0	256.5
	diff.%	0.00	0.00	0.06	0.10	-0.12	0.00

diff. % = (This study-SAP2000)×100/This study

TABLE V
THE NATURAL FREQUENCIES OF HYPERBOLOIDAL HELIX HAVING THE THIN-THICK OPEN SQUARE BOX SECTIONS WITH FIXED-FIXED BOUNDARY CONDITION

t/a		ω (in Hz)					
		1	2	3	4	5	6
0.040	this study	17.3	23.0	24.0	49.1	55.6	57.9
	SAP2000	17.3	23.1	23.9	48.9	55.4	58.5
	diff.%	0.00	-0.43	0.42	0.41	0.36	-1.04
0.125	this study	54.2	71.0	72.1	135.1	153.1	175.2
	SAP2000	54.3	71.4	71.8	134.9	152.6	176.6
	diff.%	-0.18	-0.56	0.42	0.15	0.33	-0.80
0.250	this study	108.5	134.8	137.1	261.0	300.0	324.4
	SAP2000	108.6	135.4	136.6	260.8	299.1	326.4
	diff.%	-0.09	-0.45	0.36	0.08	0.30	-0.62
0.375	this study	161.1	183.6	187.1	380.7	423.1	428.2
	SAP2000	161.4	183.8	186.7	381.3	422.0	428.5
	diff.%	-0.19	-0.11	0.21	-0.24	0.26	-0.07

diff. % = (This study-SAP2000)×100/This study

TABLE VI
THE NATURAL FREQUENCIES OF HYPERBOLOIDAL HELIX HAVING THE THIN-THICK OPEN SQUARE BOX SECTIONS WITH FIXED-FREE BOUNDARY CONDITION

| t/a		ω (in Hz)					
		1	2	3	4	5	6
0.040	this study	3.7	3.9	9.6	20.6	21.4	24.9
	SAP2000	3.7	3.9	9.6	20.6	21.3	-
	diff.%	0.00	0.00	0.00	0.00	0.47	-
0.125	this study	11.4	12.0	30.0	63.9	66.2	77.7
	SAP2000	11.4	12.1	30.0	64.0	66.1	-
	diff.%	0.00	-0.83	0.00	-0.16	0.15	-
0.250	this study	22.2	23.3	60.2	122.7	126.9	153.1
	SAP2000	22.2	23.3	60.2	123.1	126.7	-
	diff.%	0.00	0.00	0.00	-0.33	0.16	-
0.375	this study	31.4	32.6	89.8	166.8	175.3	202.4
	SAP2000	31.4	32.6	89.8	167.0	175.1	202.6
	diff.%	0.00	0.00	0.00	-0.12	0.11	-0.10

diff. % = (This study-SAP2000)×100/This study
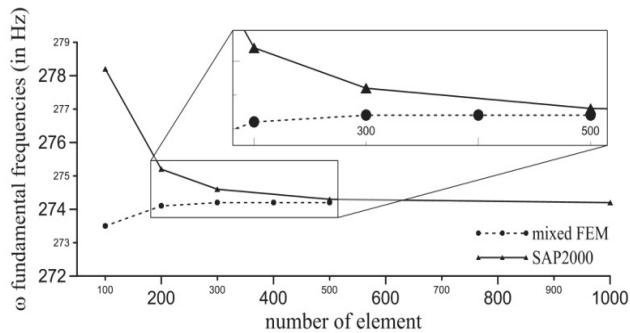
Fig. 3 The convergence analysis for ω fundamental frequency of the hyperboloidal helix having square box cross-section with fixed-fixed boundary condition

IV. CONCLUSIONS

Static and dynamic analyses of hyperboloidal helix having the thin/thick closed and open square box cross-sections are investigated via the mixed FE method. The torsional rigidity of the used cross-sections is determined by the method proposed by the authors [20]. The FE solutions are compared using the commercial program SAP2000 and its Section Designer module. The percent differences between these FE models is in range of 0-1.18% in the case of 1000 elements by SAP2000 and 200 elements by the present mixed model for both the static and dynamic analyses, and, the thin/thick closed and open square box sections. The convergence of the static and dynamic analyses of two FE analyses is given in Figs. 2, 3. In mixed FE analysis, convergence of the vertical displacement is upper bound and the fundamental natural frequency is lower bound. This difference is due to the used torsional rigidity of the cross-sections, besides the straight SAP2000 elements and the curved elements of the present study. The effects of the closed and the open square box sections that range from thin to thick with four different thickness-to-side ratios and the boundary conditions on the static and the dynamic behavior of the hyperboloidal helix are discussed extensively.

REFERENCES

[1] M.H. Omurtag and A.Y. Aköz, "The mixed finite element solution of helical beams with variable cross-section under arbitrary loading", *Comput. Struct.*, vol. 43, pp. 325–331, 1992.
[2] V. Haktanır and E. Kıral, "Statical analysis of elastically and continuously supported helicoidal structures by the transfer and stiffness matrix methods", *Comput. Struct.*, vol. 49, pp. 663–677, 1993.
[3] W. Busool and M. Eisenberger, "Exact static analysis of helicoidal structures of arbitrary shape and variable cross section", *J. Struct. Eng.*, vol. 127, pp. 1266–1275, 2001.
[4] V. Yıldırım, "Investigation of parameters affecting free vibration frequency of helical springs", *Int. J. Numer. Methods Eng.*, vol. 39, pp. 99–114, 1996.
[5] J.E. Mottershead, "Finite elements for dynamical analysis of helical rods", *Int. J. Mech. Sci.*, vol.22, pp. 267–283, 1980.
[6] J. Lee, "Free vibration analysis of cylindrical helical springs by the pseudospectral method", *J. Sound Vib.*, vol. 302, pp. 185–196, 2007.
[7] A.M. Yu, C.J. Yang and G.H. Nie, "Analytical formulation and evaluation for free vibration of naturally curved and twisted beams", *J. Sound Vib.*, vol. 329, pp. 1376–1389, 2010.
[8] N. Eratlı, M. Ermis and M.H. Omurtag, "Free vibration analysis of helicoidal bars with thin-walled circular tube cross-section via mixed finite element method", *Sigma Journal of Engineering and Natural Sciences*, vol. 33(2), pp. 200-218, 2015.
[9] S.A. Alghamdi, M.A. Mohiuddin and H.N. Al-Ghamedy, "Analysis of free vibrations of helicoidal beams", *Eng. Comput.*, vol. 15, pp. 89–102, 1998.
[10] S. Timoshenko and J.N. Goodier, *Theory of elasticity*, McGraw-Hill, New York, 1951.
[11] R.J. Roark, *Formulas for Stress and Strain*, McGraw-Hill, New York, 1954.
[12] N.X. Arutunan and B.L. Abraman, *Torsion of Elastic Bodie*s (in Russian), State Publisher, Fizmatgiz, Moscow, 1963.
[13] C.T. Wang, *Applied Elasticity*, McGraw-Hill, New York, 1953.
[14] J.F. Elyand and O.C. Zienkiewicz, "Torsion of compound bars-A relaxation solution", *Int. J. Mech. Sci.*, vol. 1, pp. 356-365, 1960.
[15] L.R. Hermann, "Elastic torsional analysis of irregular shapes", *J. Engng. Mech.*, ASCE, vol. 91(6), pp. 11-19, 1965.
[16] J.L. Krahula and G.F. Lauterbach, "A finite element solution for Saint-Venant torsion", *AIAA Journal*, vol. 7(12), pp. 2200-2203, 1969.
[17] K. Darılmaz, E. Orakdogen, K. Girgin and S. Küçükarslan, "Torsional rigidity of arbitrarily shaped composite sections by hybrid finite element approach", *Steel and Composite Structures*, vol. 7(3), pp. 241-251, 2007.
[18] Z. Li, J.M. Ko and Y.Q. Ni, "Torsional rigidity of reinforced concrete bars with arbitrary sectional shape", *Finite Elements in Analysis and Design*, vol. 35, pp. 349-361, 2000.
[19] J.S. Lamancusa and D.A. Saravanos, "The torsional analysis of bars with hollow square cross-sections", *Finite Element in Analysis and Design*, vol. 6, pp. 71-79, 1989.
[20] N. Eratlı, M. Yılmaz, K. Darılmaz and M.H. Omurtag, "Dynamic analysis of helicoidal bars with non-circular cross-sections via mixed FEM", *Struct. Eng. Mech.*, vol. 57(2), pp. 221-238, 2016.
[21] E.J. Sapountzakis, "Nonuniform torsion of multi-material composite bars by the boundary element method", *Computers and Structures*, vol. 79, pp. 2805-2816, 2001.
[22] E.J. Sapountzakis and V.G. Mokos, "Nonuniform torsion of bars variable cross section", *Computers and Structures*, vol. 82, pp. 03-715, 2004.
[23] J.T. Oden and J.N. Reddy, *Variational Method in Theoretical Mechanics*, Springer-Verlag, Berlin, 1976.